Suppression of Radical Attack in Polymer Electrolyte Membranes using a Vinyl Polymer Blend Interlayer with Low Oxygen Permeability

Zulfi Al Rasyid Gautama[a], Yasir Arafat Hutapea[b], Byungchan Hwang[b], Junko Matsuda[c,d], Albert Mufundirwa[e], Takeharu Sugiyama[f], Miho Ariyoshi[d], Shigenori Fujikawa[d], Stephen Matthew Lyth[a,d,g], Akari Hayashi[b,c,g,h], Kazunari Sasaki[b,c,d,h] and Masamichi Nishihara* [d,h]

[a] Graduate School of Integrated Frontier Science, Department of Automotive Science, Kyushu University, 744 Motooka, Nishi-ku, Fukuoka, 819-0395, Japan

[b] Graduate School of Engineering, Department of Hydrogen Energy Systems, Kyushu University, 744 Motooka, Nishi-ku, Fukuoka, 819-0395, Japan

[c] International Research Center for Hydrogen Energy, Kyushu University, 744 Motooka, Nishi-ku, Fukuoka, 819-0395, Japan

[d] International Institute for Carbon-Neutral Energy Research (I2CNER), Kyushu University, 744 Motooka, Nishi-ku, Fukuoka, 819-0395, Japan

[e] Japan Synchrotron Radiation Research Institute (SPring-8/JASRI), 1 Chome-1 Koto, Sayo, Sayo District, Hyogo, 679-5198, Japan

[f] Research Center for Synchrotron Light Applications (RCSLA), Kyushu University, 8 Chome-7 Yayoigaoka, Tosu, Saga 841-0005, Japan

[g] Platform for Inter-Transdisciplinary Energy Research (Q-PIT), Kyushu University, 744 Motooka, Nishi-ku, Fukuoka, 819-0395, Japan

[h] Next-Generation Fuel Cell Research Center (NEXT-FC), Kyushu University, 744 Motooka, Nishi-ku, Fukuoka, 819-0395, Japan

Corresponding author: Masamichi Nishihara, nishihara.masamichi.064@m.kyushu-u.ac.jp

This is a peer-reviewed, accepted author manuscript of the following paper: Gautama, Z. A. R., Hutapea, Y. A., Hwang, B., Matsuda, J., Mufundirwa, A., Sugiyama, T., Ariyoshi, M., Fujikawa, S., Lyth, S. M., Hayashi, A., Sasaki, K., & Nishihara, M. (2022). Suppression of radical attack in polymer electrolyte membranes using a vinyl polymer blend interlayer with low oxygen permeability. Journal of Membrane Science, 658, [120734]. https://doi.org/10.1016/j.memsci.2022.120734

Abstract:

Decomposition of polymer electrolyte membranes (PEMs) by radical species is a significant issue related to the chemical durability of polymer electrolyte fuel cells (PEFCs). A major contributor to radical formation is the oxygen crossover through the membrane from cathode to anode. Therefore, suppression of oxygen diffusion through the PEM is predicted to effectively mitigate the chemical degradation via radical formation. To confirm this, a simple high oxygen barrier PEM is prepared by sandwiching a thin gas barrier interlayer in between two Nafion 211 membranes. The interlayer consists of poly(vinyl alcohol) (PVA) and poly(vinyl sulfonic acid) (PVS) with various molar ratio. The sandwich PEM can show 286 times lower oxygen permeability than Nafion 212 membrane, which corresponds to 1.7 times longer survival time than Nafion 212 in a chemically accelerated stress test for PEMs known as open circuit voltage (OCV) holding test. Furthermore, the SEM image of the sandwich PEM cross-section shows that the interlayer could survive the OCV holding test despite its lower resistance against radical attack. The results in this study indicate that the addition of high oxygen barrier interlayer can reduce radical formation in PEFC and improve chemical durability.

Keywords:

Fuel cell, polymer electrolyte membrane, oxygen permeability, Polyvinyl alcohol, OCV holding test

1. Introduction

Polymer electrolyte fuel cells (PEFCs) efficiently generate a voltage via electrochemical reaction between hydrogen and oxygen, emitting only water and heat as byproducts [1,2]. Consequently, they have huge potential for the decarbonization of e.g. the automotive industry by replacing combustion engines and fossil fuels. However, several technical problems remain, and these should be solved to assist with the wider commercialization of PEFCs. One of the key components in a PEFC is the polymer electrolyte membrane (PEM). The PEM facilitates proton transport from anode to cathode, acts as an electron insulator to prevent short circuiting, and prevents the mixing of hydrogen and air either at the anode or cathode[2].

A major problem with PEMs is chemical degradation. During PEFC operation, radical species (i.e. ·OH and ·OOH) can be generated through reaction between oxygen and hydrogen in the presence of platinum. These radicals attack the chemical bonds of PEMs, resulting in degradation via membrane thinning and in the extreme case, pinhole formation[3]. Consequently, perfluorosulfonic acid (PFSA) polymers such as Nafion are used as a PEM material partly due to the presence of strong C-F bonds in the main chain. However, PFSAs have several drawbacks, including: high cost[4]; hazardous and ecologically damaging synthesis procedures[5]; and poor stability at high operating temperature (e.g. >90 °C)[6].

Hydrocarbon-based PEMs can overcome some of these limitations due to their low cost[7–9], simple and varied synthesis procedures[10,11], and their stability at elevated temperature[12,13]. However, hydrocarbon PEMs generally suffer from lower chemical durability compared to PFSA PEMs[14]. To tackle this issue, two main strategies have been developed to date. The first is the development of chemically durable hydrocarbon polymers that can resist radical attack. For example, sulfonated poly(phenylene) has surpassed the chemical durability of Nafion in open-circuit voltage (OCV) holding tests[15,16]. The second strategy is to implement radical scavenging additives into the hydrocarbon PEM[17–19]. For example, sulfonated poly(ether sulfone) impregnated with cerium oxide was able to survive four times longer compared to Nafion membranes in OCV holding tests[20].

Although higher chemical durability than Nafion has already been achieved by hydrocarbon PEMs, further improvements are still necessary to produce more durable PEMs for practical applications. Despite this, current strategies appear to have almost reached their performance limit, and therefore, new concepts in PEM design are necessary. As an alternative “third” strategy, we therefore focus here on the mechanism of chemical degradation in PEMs.

As mentioned above, chemical degradation is mainly caused by radicals generated from the reaction of hydrogen and oxygen on the Pt catalyst[21]. In addition, the reaction can also occur through the decomposition of hydrogen peroxide, especially in the presence of metal contaminants[22]. Some radical formation mechanisms have been

reported[23–28], as summarized in Fig. 1. One of the mechanisms involves the permeation of oxygen through the PEM from the cathode to the anode, where it reacts with hydrogen on the Pt catalyst[23–25]. Another mechanism involves the two-electron oxygen reduction reaction at the cathode Pt catalyst[26–28]. In addition to these major mechanisms, some literatures also reported that chemical degradation happens at the Pt band in the PEM[29,30]. From the reported mechanisms, oxygen permeation through the PEM plays an important role in radical formation.

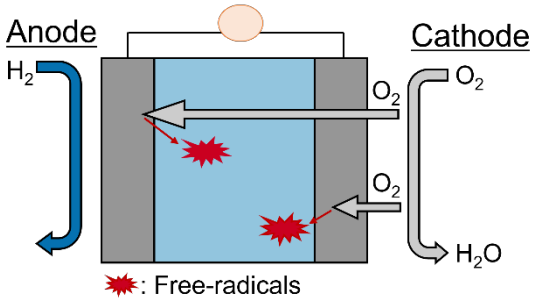

Fig. 1. Schematic diagram of radical formation in PEFC operation. (I) radical formation by permeated oxygen from cathode through PEMs, (II) radical formation through two-electron reduction reaction at cathode

As such, suppressing oxygen diffusion through the membrane is likely be highly effective in mitigating chemical degradation via radical formation. In this study, we aim to achieve this by incorporating an oxygen barrier layer in the PEM. Poly(vinyl alcohol) (PVA) is a common polymer which is well-known for its gas barrier properties. Indeed, the oxygen permeability of PVA in dry conditions at 35°C is reported to be 1.5×10^{-3} Barrer[31], or around 500 times lower than Nafion 212, measured under similar conditions (i.e. 8.1×10^{-1} Barrer)[32]. PVA also has the added advantages of being extremely cheap[33], with good membrane formability, and is biodegradable. On the other hand, PVA has very low proton conductivity compared to Nafion, and is soluble in water[33–36]. Several reports have investigated PVA in fuel cell applications. For example, Sahu et al. reported a 10-fold increase in proton conductivity by blending PVA with 35 wt% poly(styrene sulfonic acid) (PSSA), and used crosslinking to improve the stability in water[36]. In other work, Kim et al. blended vinylon (a PVA-derived polymer) with PFSA and laminated the resulting membrane with Nafion, fabricating in a thin (10 μm) sandwich PEM with improved PEFC performance compared to a pure Nafion membrane[37]. However, to the best of our knowledge the chemical durability of PVA-based membranes in OCV holding tests has not been reported, presumably because of poor stability against radical attack[34,35].

Here, we aim to confirm if the addition of an oxygen barrier can improve the chemical durability of a PEM. PVA is used as an oxygen barrier, and this is blended with poly (vinyl sulfonic acid) (PVS) to improve the proton conductivity. Sandwich PEM structures are fabricated by incorporating a thin layer of PVA/PVS between two Nafion 211 membranes (Fig 2). The resulting PEMs subjected to OCV holding tests to assess the chemical durability.

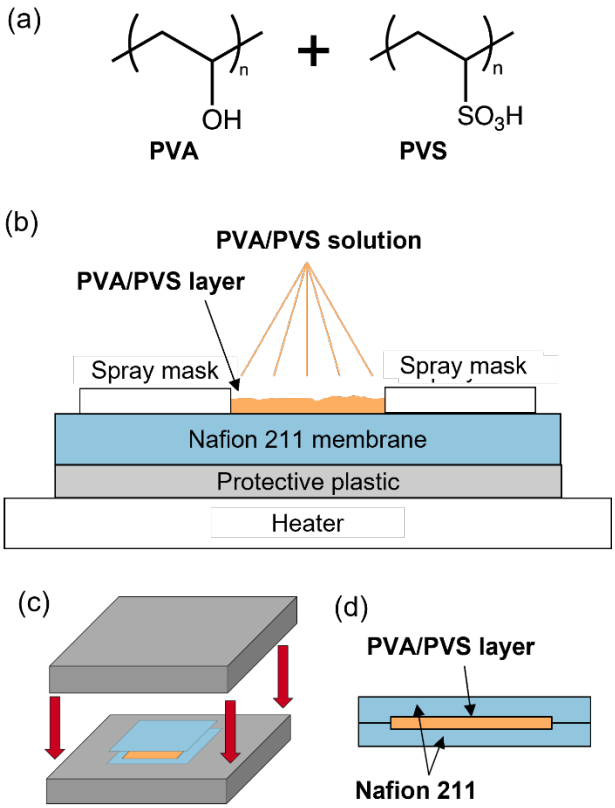

Fig 2. Sandwich PEM preparation method. (a) Polymer blending of PVA and PVS in aqueous solution, (b) spray process of PVA/PVS solution, (c) hot press process and (d) Sandwich PEM structure consisting PVA/PVS inner layer and two Nafion outer layers,

2. Experimental Section

2.1 Chemicals and materials

Poly(vinyl alcohol) (PVA) pellets (fully hydrolyzed, Mw. 60,000, Merch Schuchardt, Germany) were used for membrane preparation. Poly(vinyl sulfonic acid, sodium salt) (PVSNa) 25 wt% aqueous solution (Sigma Aldrich, USA) was acidified by mixing with DIAION™ Ion Exchange Resin (Mitsubishi Chemical Corporation) for 3 h at least 5 times to obtain poly (vinyl sulfonic acid) (PVS) solution. Nafion 211 and Nafion 212 (DuPond), Nafion 5 wt% solution (Wako Chemicals), ethanol 95% (Wako Chemicals), platinum-decorated ketjen black (Pt-KB, Tanaka Kikinzoku Kogyo K.K., 46.8 wt% Pt), and gas diffusion layers (GDLs, EC-TP1-060T, TOYO Corporation) were used for membrane-electrode assembly (MEA) preparation and several measurements. Other solvents and chemicals were purchased from Wako chemicals and used without further purification.

2.2 Preparation method of sandwich PEMs and stand-alone PVA/PVS membranes

First, PVSNa was protonated by using DIAION resin in DI water to obtain PVS solution. The PVS solution was mixed with PVA aqueous solution with various molar ratios shown in Table 1. Then, the interlayer was prepared by spraying PVA/PVS solution onto the surface of a Nafion 211 membrane (9 cm^2) heated to 60°C, using a spray gun (Tamiya, Spray-work HG, wide airbrush, trigger type) connected to an air compressor (Tamiya, HG air compressor, Revo II) (Fig. 2(b)). The required volume of PVA/PVS solution was determined based on the deposited polymer weights on Nafion 211. A plastic spray mask was used to control the sprayed area to 4 cm^2. The pressure valve of the spray gun was adjusted so that the water evaporated immediately after deposition. Next, a second layer of Nafion 211 was placed on top of the PVA/PVS sprayed Nafion 211, then hot pressed (Sinto) together at 132 °C and 0.3 kPa for 3 min (Fig. 2 (c)). The obtained sandwich structure has the PVA/PVS layer encapsulated by Nafion 211 membranes (Fig. 2 (d)). In addition to sandwich PEMs, free-standing PVA/PVS membranes (Table 1) were also prepared by depositing 8 mg/cm^2 of PVA/PVS solution on a plastic substrate to characterize the interlayer.

Table 1 Summary of the sandwich PEMs and PVA/PVS membranes prepared in this study.

Sample name	Molar ratio (PVA:PVS) -	Areal density of interlayer mg/cm^2	Thickness μm	Ion Exchange Capacity meq/g	Oxygen permeability Barrer
Nafion 212	-	-	50	0.97	9.97
PVA/PVS 1	1:1	8	~20-	3.10	-
PVA/PVS 10	10:1	8	~20	1.88	-
PVA/PVS 100	100:1	8	~20	0.12	-
S1-0.5	1:1	0.5	49	-	-
S10-0.5	10:1	0.5	48	-	-
S20-0.5	20:1	0.5	49	-	0.21
S60:0.5	60:1	0.5	49	-	0.1
S100-0.5	100:1	0.5	48	-	0.03
S100-0.3	100:1	0.3	48	-	1.05
S100-0.1	100:1	0.1	47	-	2.23

2.3 MEA preparation

For MEA preparation, a catalyst ink solution was prepared from Pt/C electrocatalyst powder (Pt: 46.8 wt%), Nafion 5 wt% solution, deionized water, and ethanol. These materials are mixed to obtain a catalyst ink that yields to 28 wt% of Nafion ionomer in the electrocatalyst layer. The catalyst ink was then coated onto both sides of the membrane using a spray machine (Nordson, K.K.) to obtain 1 cm^2 electrode surface with 0.3 mg Pt loading. The sprayed membrane was hot pressed at 0.3 MPa and 132 °C for 180 seconds (SINTO CYPT-1, Japan) resulting in a catalyst coated membrane (CCM). This was sandwiched between two GDLs to obtain an MEA, which was then mounted in a Japan Automotive Research Institute (JARI) cell with 1 cm^2 electrode area, forming a fuel cell assembly.

146

147 *2.4 Instrumental characterization*

148 X-ray Diffraction (XRD) pattern of free-standing membranes were obtained from a SmartLab 9kW AMK X-ray
149 Diffractometer (Rigaku, Japan) with Cu Kα (1.54 Å). The characteristic distance (corresponding in this case to the
150 distance between polymer chains) was calculated using the Bragg's law.

151 Small Angle X-ray Scattering (SAXS) was performed at beamline BL-06 of The SAGA Light Source, Saga, Japan.
152 The x-ray energy used was 9 keV (λ = 1.38065 Å) with a monochromator resolution, DE ~0.9eV. Silicon nitrate was
153 used as a sample window with a camera path length of 1087.201 mm. The scattering patterns were detected using
154 Dectris Pilatus 3 300K with the area detector of 172 μm × 172 μm pixel size. The free-standing membranes were
155 hydrated for 60 minutes before measurement, and the cluster size was measured using the Bragg's law.

156 The ion exchange capacities (IECs) of the free-standing membranes were obtained by acid-base titration. First, the
157 membranes were dried obtaining their weights. Then, the membranes were immersed in 1 M NaCl solution for 24 h,
158 then the HCl content in the solution was titrated using 0.01 M or 0.001 M NaOH and phenolphthalein as a pH indicator.

159 Oxidative stability of the stand-alone membranes was investigated via immersion in Fenton's solution (3 wt% H2O2,
160 4 ppm Fe^{2+} ion) at 80°C. After immersion, the membranes were dried before obtaining their weights. The PVA/PVS
161 membranes were completely dissolved after immersion, so PVA solution (50 mg/ml) was mixed with the Fenton's
162 solution at 80°C to investigate the oxidative stability. The change of molecular weight of PVA solution before and after
163 Fenton's test was investigated by gel permeation chromatography (GPC) at 40°C (Eluent, DMSO with 0.01 M LiBr;
164 columns, TSK gel SuperAW; detector, JASCO UV 2075 Plus).

165 The cross-sections of the membranes were observed using Scanning Electron Microscope (SEM) and energy
166 dispersive X-Ray spectroscopy (EDS) in Versa 3DLV (FEI™) with 10 kV acceleration voltage. Prior to measurement,
167 PEMs were fixed in resin and left overnight to cure. Then, a flat cross-section was obtained by microtome (Leica EM
168 UC6). Subsequently, the sample surface was sputter coated with gold under 5 Pa pressure and 0.8 V for 3 minutes (SC-
169 701 MkII ECO, Sanyu Electron). The distance between the sample surface and the objective lens was adjusted to 10
170 mm.

171 Through-plane proton conductivity was determined by electrochemical impedance spectroscopy on MTS-740
172 (Scribner associates Inc., US) at 80°C and varying relative humidity. The impedance spectra were measured using a
173 Solartron SI-1260 under current loading of 0.1 mA, applied voltage of 1 V, and a frequency range of 1 to 5 MHz. The
174 proton conductivity of polymer electrolyte membranes was determined by the x-intercept of Nyquist plots using the
175 following equation,

176

$$\sigma = t/RA \quad (1)$$

where t is the thickness of the membrane, R is the resistance in the high frequency region obtained from the impedance spectra (i.e. the intercept of the X axis), and A is the contact area of the measurement electrodes (0.5 cm^2). The resistance of the sandwich PEMs was initially too low to measure by electrochemical impedance spectroscopy using the available setup. Therefore, two identical sandwich PEMs were attached to each other by hot pressing at 132°C and 0.3 kPa for 3 mins before measuring the proton conductivity. The thickness after hot pressing was used as the thickness of the membrane, t.

Oxygen and hydrogen permeability tests of the sandwich PEMs were measured on GTR-11A/31A gas barrier testing system (GTR Tec corp., Japan). The surface area of the samples was set to 0.8 cm^2. To measure the gas permeability, the feed gas was pressurized to 100 kPa, while the permeate side was held at -100 kPa, resulting in a total pressure differential of 200 kPa. The temperature for the measurement was 80°C without humidity control. The volume of the permeated gas was measured via gas chromatography (TCD, G3700T, Yanaco, Kyoto, Japan). The gas permeability was measured using the following equation,

$$P = v/(l \cdot A \cdot r \cdot \Delta p) \quad (2)$$

where P is the gas permeability, v is the permeated volume of gas, l is the thickness of the sample, A is the area of the sample (0.8 cm^2), t is the measurement time and Δp is the pressure difference (200 kPa).

Fuel cell evaluation and OCVs holding test were carried out using an AUTOPEM-CVZ01 (Toyo Corporation, Japan) connected to a potentiostat (SI-1287) and a frequency analyzer (SI-1255B). For the evaluation of fuel cell performance, the cell temperature and relative humidity were maintained at 80°C and 95% RH, respectively. The measurement of polarization curves was carried out by potential sweeping from the OCV to 0.2 V with a 20 mV/s scan rate, under 139 mL/ min hydrogen flow at the anode, and 332 mL/min air flow at the cathode. The hydrogen crossover current density measurements were performed by potential sweeping from 0.2 V to 0.5 V at 5 mV/s under 70 mL/min hydrogen flow at the anode, and 166 mL/min nitrogen flow at the cathode. The cell resistance was determined from the average measurement of impedance spectroscopy under 0.05 A, 0.1 A, and 0.2 A direct current loading using the frequency analyser. The OCV holding test was performed by maintaining OCV conditions at 90°C and 30% RH, under 139 mL/min hydrogen flow at the anode, and 332 mL/min air flow at the cathode. After each 72 h during OCV holding test, the temperature and relative humidity was changed to 80°C and 95% RH for fuel cell evaluation using the above

procedure. The OCV holding test was continued until the measured hydrogen crossover current density was 10 times higher than the initial value.

3. Results

3.1 Structural Analysis of PVA/PVS membranes

The effect of varying the molar ratio on free-standing PVA/PVS membranes was investigated using X-ray diffraction (XRD), as summarized in Fig. 3 (a). The characteristic peak of the PVA/PVS polymer blend occurs at a larger 2q (~20°) than Nafion 212 (17°), which corresponds to a shorter average distance between each polymer chain in the PVA/PVS membranes is smaller (~0.44 nm) than Nafion 212 (~0.52 nm). This can be explained by the fact that the PVA/PVS membrane has a greater degree of hydrogen bonding than Nafion 212, due to the presence of hydroxyl groups, allowing the polymer chains to reside closer together[38]. A shorter distance between polymer chains reduces the free volume, decreasing gas permeation and improving the gas barrier properties. The incorporation of PVS does not significantly affect the inter-chain distance, but the intensity of the characteristic peak increases as the molar ratio of PVA increases, indicating that PVA is mainly responsible for the changes in crystal structure[39]. Meanwhile, the presence of sulfonic acid groups in PVS is reported to hinder the crystallization of PVA through intermolecular

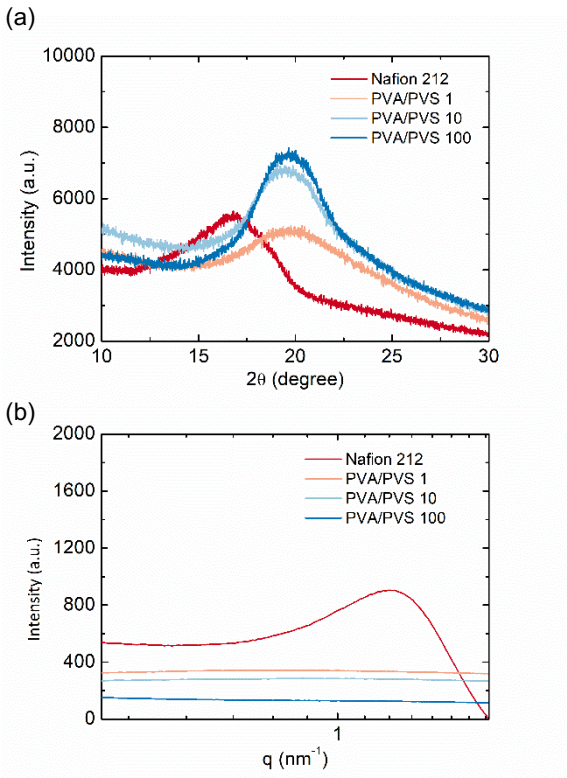

Fig. 3. Characterization of polymer structure of Nafion 212 and free-standing PVA/PVS membranes. a) XRD and b) SAXS.

interaction [40]. High crystallinity is desirable for gas barrier applications because this lengthens the gas diffusion pathway.

Small angle X-ray scattering (SAXS) measurements can reveal information about the size of hydrophilic domains in PEMs, which generally correspond to proton conduction pathways[13,41–43]. As such, SAXS was performed on a Nafion 212 reference membrane, and on free-standing PVA/PVS membranes, as shown in Fig. 3 (b). For Nafion 212, a clear crystalline peak is observed at around 1.2 nm^{-1} [41–43]. However, in the case of the PVA/PVS membranes, no such peak is observed. This indicates that the PVA/PVS membranes are amorphous and uniformly mixed, with no phase-separated proton pathway[13].

3.2 SEM and EDS observation of the sandwich PEM

After the fabrication of sandwich PEMs, the cross-sections of the PEMs were characterized by SEM and EDS. The SEM image of S100-0.5 in Fig. 4 (a) confirms the successful introduction of the PVA/PVS interlayer between the Nafion 211 membranes, with a uniform thickness of around 2.2 μm. EDS mapping shows a high er concentration of carbon and a lower concentration of fluorine running through the center of the sandwich PEM, corresponding well with the un-fluorinated hydrocarbon PVA/PVS interlayer (Fig. 4 (b), (c)). The cross-sectional images of the other S100-0.1

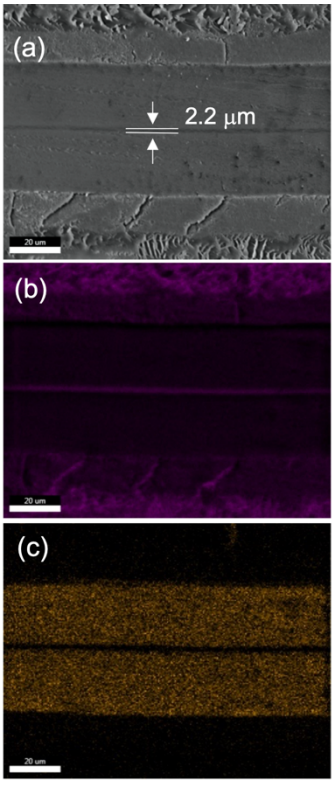

Fig. 4. SEM and EDS analysis of S100-0.5 cross-section with (20 μm scale bar). (a) SEM image before OCV holding test. Elemental analysis before OCV holding test for (b) carbon and (c) fluorine.

and S100-0.3 membranes with different areal density can be found in the Supplementary Information (Fig. S1). The corresponding thicknesses are 0.5 µm and 1.1 µm for S100-0.1 and S100-0.3, respectively. This confirms that the interlayer thickness can be controlled by varying the areal density.

3.3 Proton conductivity

Fig. 5 shows the proton conductivity of the sandwich PEMs at 80°C and different relative humidity. At 95% relative humidity, the measured proton conductivity of Nafion is ~170 mS/cm. This is considerably higher than the reported values of Nafion membranes (~100 mS/ cm)[44,45] and this is attributed to the hot pressing used prior to the measurement. High temperature treatment has previously been reported to improve the proton conductivity of Nafion membranes by increasing the proportion of hydrophilic clusters, allowing better water uptake and enhanced proton diffusion[46–48]. Meanwhile, sandwich membranes have lower proton conductivity, which is dependent on the molar ratio of PVS in the interlayer. S1-0.5 has the highest proton conductivity (~90 mS/cm), followed by S10-0.5 (~85 mS/cm), and S100-0.5 (~50 mS/cm). Interestingly, the proton conductivity of Nafion was higher than all sandwich PEMs even in the case that the interlayers have higher ion exchange capacity (IEC), namely 3.10 meq/g for S1-0.5 and 1.88 meq/g for S10-0.5 (Table 1). One possible explanation for this is that PVA/PVS does not have a phase-separated proton pathway like Nafion 212, as confirmed by SAXS (Fig. 3 (b))[41,43]. Another is increased membrane resistance due to the interfaces between the PVA/PVS interlayer and the two Nafion layers. This may be compounded by the highly dissimilar nature of the polymers in the different layers.

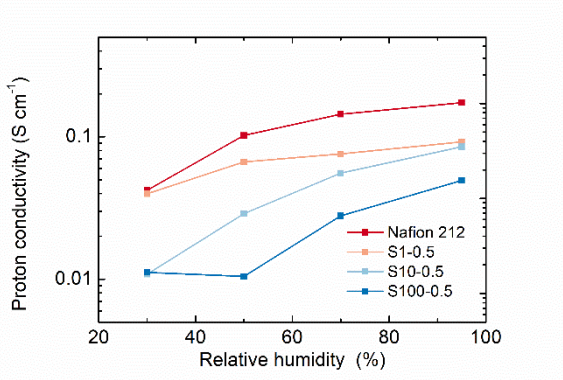

Fig. 5 Proton conductivity of Nafion and sandwich PEMs at 80°C under varying relative humidity

3.4 Oxygen permeability

The motivation for incorporation of a PVA/PVS interlayer in the PEM is to enhance the chemical durability by acting as an oxygen barrier. Therefore, the oxygen permeability was measured at 80˚C, simulating PEFC operating conditions. All the sandwich PEMs displayed significantly lower oxygen permeability compared to the pure Nafion 212 membrane, and the oxygen permeability decreased with increasing molar ratio of PVA in the interlayer (Fig. 6 (a), Table 1). The lowest oxygen permeability was obtained for S100-0.5, with a value of 3.5×10-2 Barrer, which is 286 times lower than Nafion 212 (1.0×101 Barrer). Therefore, it is concluded that the PVA/PVS interlayer successfully acts as an oxygen barrier, and a molar ratio of 100:1 is the most effective oxygen barrier. Since the main purpose of this study is to investigate the effect of using an oxygen barrier on the chemical durability of PEMs, this molar ratio was selected for OCV holding tests in the next section, despite the relatively low proton conductivity (Fig. 5).

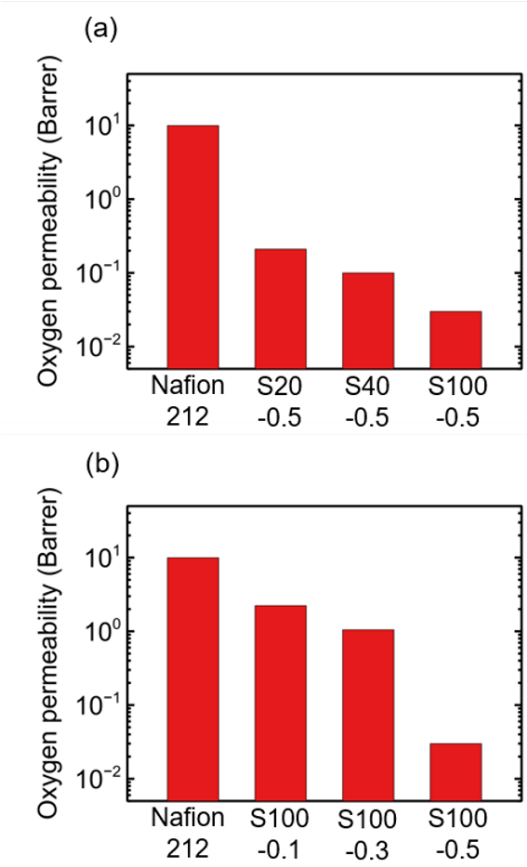

Fig. 6. Oxygen permeability of Nafion 212 and sandwich PEMs measured at 80 ºC. (a) Different PVA and PVS molar ratio and (b) different areal density of the deposited PVA-PVS layer.

Next, the effect of changing the areal density (i.e. varying the thickness) of the PVA/PVS interlayer on the oxygen barrier properties was investigated (Fig. 6 (b)). Areal densities of 0.5, 0.3 and 0.1 mg/cm^2 correspond to thicknesses of 2.2 µm, 1.1 µm and 0.5 µm, respectively (Fig. 4 (a), S1). Increasing the thickness significantly decreases the oxygen permeability, by almost two orders of magnitude, as expected due to conventional diffusion relations. Accordingly, an areal density of 0.5 mg/cm2 was selected for the OCV holding tests in the next section.

3.5 Fuel Cell Performance and OCV holding tests

To confirm the effect of adding an oxygen barrier, fuel cells were assembled using the sandwich PEMs, and polarization curves were measured (Fig. 7 (a)). This confirmed that sandwich PEMs can be successfully employed in fuel cells, although the performance is currently lower than that of Nafion.

In this study, the main purpose is to clarify the effect of incorporating an oxygen barrier layer on the chemical degradation of PEMs. As such, the sandwich PEM with lowest oxygen permeability (S100-0.5) was selected for open circuit voltage (OCV) holding tests, despite having lower proton conductivity and fuel cell performance compared to the other sandwich PEMs. The fuel cell with the S100-0.5 membrane survived for 333 hours in the OCV holding test before failure, with an average voltage drop of 1.27 mV/h (Fig. 7 (b)). Meanwhile, Nafion 212 survived for only 195 hours, with a much faster voltage drop of 2.11 mV/h. This result clearly confirms that incorporating an oxygen barrier layer can significantly improve the stability of PEMs against chemical degradation. In addition, hydrocarbon membranes are not generally very durable, and to the best of our knowledge this is the first example of a simple vinyl hydrocarbon polymer membrane surviving for a significant amount of time at OCV. This is possible due to encapsulation between the Nafion membranes.

In-situ measurement of oxygen crossover current density during PEFC operation has been reported[49]. However, that method requires subjecting the fuel cell to high voltage, and as a result, degradation of both the PEM and the cathode catalyst layer should be considered. On the other hand, it has been reported that hydrogen crossover current density and oxygen crossover current density display similar trends with regards to the PEM gas barrier properties[32]. Therefore, we here apply hydrogen crossover current density measurements throughout the OCV holding tests as an indicator of how the gas permeability is affected by the inclusion of an interlayer, as has been proposed by New Energy and Industrial Technology Development Organization (NEDO) and U.S Department of Energy (DOE)[50,51]. In this study, we followed NEDO protocols for OCV holding tests[50], which end when the higher hydrogen crossover current density increases by a factor of 10 relative to the initial value.

At the beginning of the OCV holding test, the initial hydrogen crossover current density for the fuel cell containing the S100-0.5 sandwich PEM is 1.36 mA/cm2 (compared with 2.00 mA/cm2 for Nafion 212). This confirms that the sandwich PEM has improved gas barrier properties (Fig. 7 (c)). Furthermore, as the OCV holding test progresses, the hydrogen crossover current density consistently remains below 2 mA/cm2 even up to 330 hours. At 333 hours, the hydrogen crossover current density suddenly increases to around 10 mA/cm2, likely indicating irreversible damage to the PVA/PVS interlayer. On the other hand, the hydrogen crossover current density of Nafion 212 rapidly increases

303 throughout the OCV holding test to almost 100 mA/cm2 at 200 hours, indicating much faster chemical degradation
304 compared to S100-0.5.

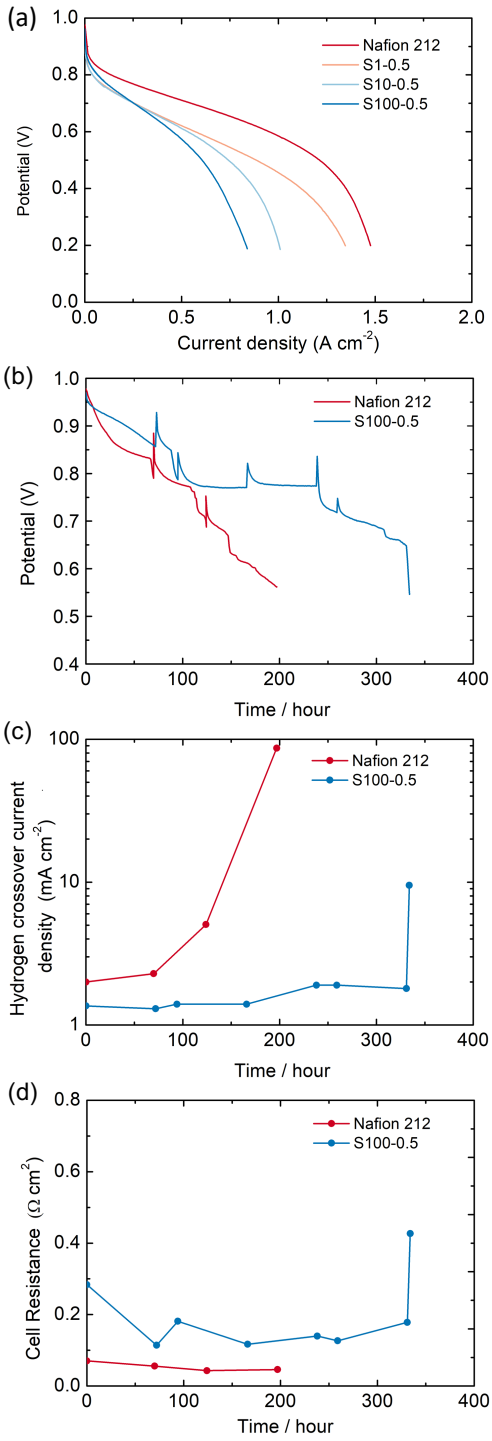

Fig. 7. Polarization curves and OCV holding test results. (a) Polarization curves at 80 °C and 95% RH, (b) OCV holding test at 90°C and 35% RH, (c) hydrogen crossover current density by LSV at 80°C and 95% RH, and (d) resistance of each MEA at 80°C and 95% RH.

305

These results indicate that the use of a gas barrier can significantly decelerate membrane degradation during fuel cell operation. In addition, the incorporation of PVA/PVS in the membrane results in hydrogen crossover current meeting the DOE target of 2 mA/ cm2[51], even well into OCV holding tests.

3.6 Cell resistance during OCV holding test

The cell resistance was also monitored during OCV holding test as another parameter to evaluate the condition of the membrane (Fig. 7 (d)). Two behaviours related to radical attack have been proposed for changes in membrane resistance during OCV holding tests. The first is membrane thinning leading to the decrease of the resistance[52], and the second is decomposition of the proton conducting sulfonic acid groups, leading to increased resistance[53]. In the case of Nafion 212, there is a small decrease in resistance during the OCV holding test. This could indicate either a small degree of membrane thinning, or a combination of the competing effects of membrane thinning and decomposition of the sulfonic acid groups.

In the case of S100-0.5, the initial cell resistance is slightly higher than for Nafion, as expected due to the lower proton conductivity. Like the case of Nafion, the cell resistance is also relatively stable up to 330 hours (with a slight decrease up to 259 hours), although a greater degree of fluctuation is observed. This again suggests either a small degree of thinning or competing effects of thinning and sulfonic acid group decomposition. After 333 hours, the cell resistance suddenly increased, possibly indicating serious damage to the PVA/PVS interlayer. The precise degradation mechanism of the interlayer is discussed in a later section. In general, hydrocarbon vinyl polymers decompose readily in the presence of radical species[54], and therefore the increase in cell resistance (and hydrogen crossover current density) may be attributed to an eventual increase in the presence these species near the interlayer.

To support this hypothesis, we carried out Fenton's test on Nafion and PVA/PVS membranes (Table S1). After the test, Nafion 212 displayed no significant weight change, while PVA/PVS decomposed completely. In addition, the molecular weight of PVA decreased by 80% after 1 hour of Fenton's test (Fig. S2), confirming that PVA is much weaker against radical attack compared to Nafion.

3.7 SEM-EDS analysis after OCV holding tests

To further elucidate the degradation mechanisms in S100-0.5 and Nafion 212 membranes, SEM and EDS analysis of the cross-sections were performed after OCV holding tests (Fig. 8). SEM images reveal that after 195 hours, the conventional Nafion 212 PEM decreases in thickness from 48 μm to 31 μm indicating that it has undergone membrane thinning at a rate of 87 nm/h (Fig. 8 (a)). Meanwhile, the thickness of the S100-0.5 sandwich PEM decreased from 50 μm to 40 μm after 200 hours, corresponding to a thinning rate of just 50 nm/h (Fig. 8 (e)). As explained in the

introduction, the main mechanism of membrane thinning is oxygen diffusion resulting in radical attack. Therefore, the slow thinning rate of the sandwich PEM indicates that the PVA/PVS interlayer successfully slows radical formation.

After 333 hours of OCV holding, it is clearly observed that membrane thinning in the sandwich PEM mainly occurs at the anode side (Fig. 8 (i)). Although PVA/PVS slows down oxygen diffusion from the cathode, eventually some oxygen molecules will reach the anode side, combining with hydrogen at the anode to form radical species, and accelerating membrane thinning.

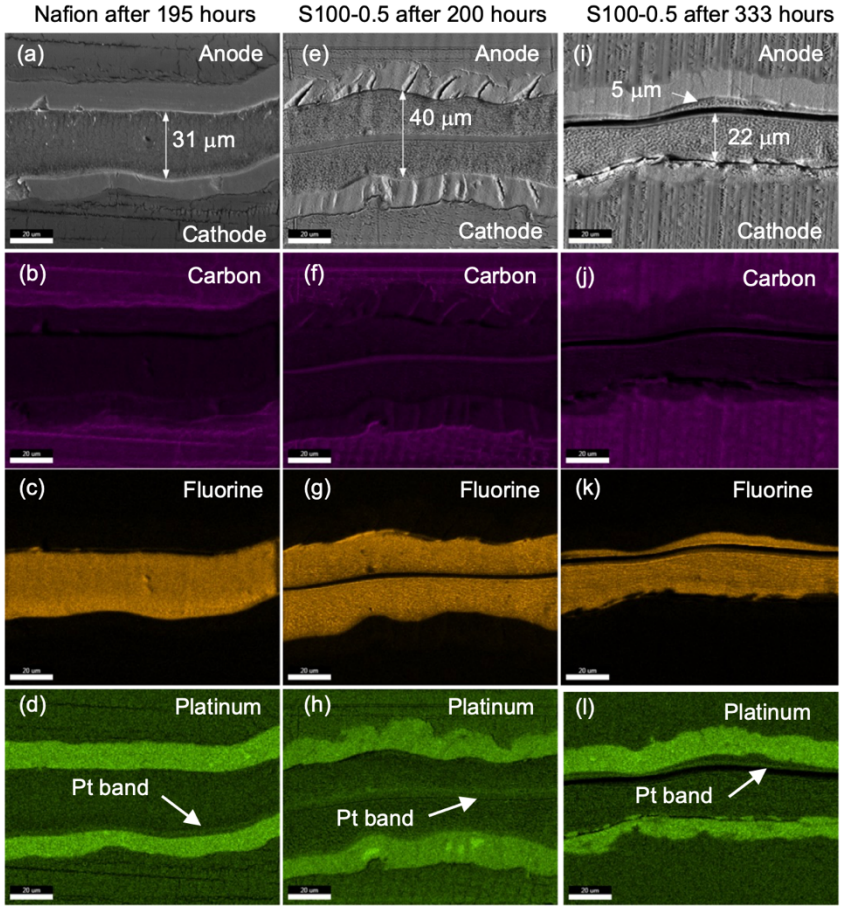

Fig. 8. SEM images and EDS analysis of the MEA cross-section after OCV holding tests (20 μm scale bar). (a)-(d) Nafion 212 after 195 h. (e)-(h) S100-0.5 after 200 h. (i)-(l) S100-0.5 after 333 hours. (b), (f), (j) are elemental carbon maps; (c), (g), (k) are elemental fluorine maps; (d), (h), (l) are elemental platinum maps showing the distribution from EDS analysis.

Furthermore, the PVA/PVS interlayer undergoes severe decomposition after 333 hours, supporting the drastic increase in cell resistance (Fig. 7 (d)). This may occur due to reasons such as radical attack to the interlayer, weakened Nafion-interlayer boundary (due to dissolution of PVA and PVS in water), or degradation near the Pt band.

Meanwhile, EDS mapping of carbon and fluorine confirms that the PVA/PVS interlayer is still intact after 200 hours. This is visible as a bright stripe through the center of the membrane in the carbon map, or a dark stripe in the fluorine map (Fig. 8 (f), (g)). This result confirms that encapsulation of the normally water-soluble PVA/PVS interlayer between

Nafion membranes effectively protects it from dissolution. It also confirms that the PVA/PVS interlayer, which is normally weak against radical attack, effectively suppresses radical formation compared to Nafion 212.

EDS mapping was also performed for platinum. As reported in previous studies[29,30], a platinum band is commonly formed in PEMs in the region where platinum ions diffusing from cathode are reduced to metallic platinum by hydrogen molecules diffusing from the anode. This process is in competition with oxidation of the platinum particle by oxygen molecules. As such, the balance between oxygen flux and hydrogen flux is important.

Here, in the case of Nafion 212, the platinum band forms close to the cathode (Fig. 8 (d), S3 (a)). This is because hydrogen molecules diffuse through the Nafion membrane much faster than oxygen molecules[32], creating a balance of hydrogen and oxygen flux near the cathode[29,30]. In contrast, in the case of the sandwich PEM, the platinum band is located on the anode side, near the interface between the PVA/PVS interlayer and Nafion (Fig. 8 (h), (l), S3 (b)). This is because the PVA/PVS interlayer suppresses both hydrogen and oxygen diffusion. As such, although hydrogen molecules still diffuse faster than oxygen molecules, the hydrogen flux through the interlayer becomes lower than the oxygen flux through Nafion membrane on the cathode side. Consequently, the entire thickness of the Nafion membrane on the cathode side is an oxidizing environment, allowing platinum ions to migrate all the way to the interlayer. It was initially predicted that the platinum band will form closer to the cathode side than the observed Pt band position due to the faster diffusion of hydrogen molecule than oxygen molecule in the interlayer (Table S2). However, the EDS mapping shows that the Pt band is formed closer to anode side. This indicates that the permeated hydrogen through the interlayer is not enough to form the Pt band on the cathode side, and the platinum ions are reduced at the boundary between Nafion and the interlayer at anode side. As such, the location of the platinum band supports the fact that the PVA/PVS layer suppresses gas diffusion.

4. Conclusions

It was hypothesized that the use of an oxygen barrier layer could suppress chemical degradation in PEMs by minimizing radical attack. To confirm this, sandwich PEMs were fabricated, incorporating a thin PVA/PVS interlayer (with low oxygen permeability) encapsulated between two Nafion 211 membranes, as described in the materials and method section. Using OCV holding tests, it was confirmed that this sandwich structure could significantly suppress chemical degradation compared to a conventional Nafion PEM, shown in the result section. The sandwich structure used in this study is particularly useful, allowing encapsulation of polymers with high gas barrier, which have hitherto not been considered in PEM applications, due to e.g. water solubility, or weakness against radical attack. The result in this work is the first example of a simple vinyl hydrocarbon polymer membrane surviving for a significant amount of time at OCV.

Despite remarkable chemical durability of the sandwich PEMs presented in this work, some technical issues remain. For example, the initial fuel cell performance should be improved, and the durability against other accelerated stress tests (such as wet-dry cycling) should be investigated. Furthermore, the investigation of oxygen crossover under humid conditions is also of interest for clarifying the gas barrier properties in realistic fuel cell conditions.

Author Contributions

Zulfi A. R. Gautama: Conceptualization, Methodology, Investigation, Writing original draft, **Yasir A. Hutapea:** Conceptualization, Methodology, Investigation, **Byungchan Hwang:** Methodology (fuel cell performance), Investigation, **Junko Matsuda:** Methodology (SEM), **Albert Mufundirwa:** Methodology (SAXS), **Takeharu Sugiyama:** Methodology (SAXS), **Miho Ariyoshi:** Methodology (gas permeability), **Shigenori Fujikawa:** Methodology (gas permeability), **Stephen M. Lyth:** Supervision, Methodology, Writing-Reviewing& Editing, **Akari Hayashi:** Methodology, Writing-Reviewing& Editing, **Kazunari Sasaki:** Methodology, Writing-Reviewing& Editing, **Masamichi Nishihara:** Supervision, Conceptualization, Methodology, Investigation, Fund acquisition, Writing-Reviewing& Editing.

Conflicts of interest

Authors declare that they have no competing interests.

Acknowledgements

The authors gratefully acknowledge financial support by the research grant of the Toyota Mobility Foundation 2019 and “Center of Innovation Science and Technology based Radical Innovation and Entrepreneurship Program (COI Program), JST Japan. The SAXS experiments were performed at Kyushu University Beamline (SAGA-LS/BL06) with the proposals of No. 2020IIIK003 and 2021IK001.

410 ## References

411 [1] S.M. Lyth, A. Mufundirwa, Electrocatalysts in Polymer Electrolyte Membrane Fuel Cells, in: W.Y. Teoh, A. Urakawa,
412 Y.H. Ng, P. Sit (Eds.), Heterogeneous Catalysts, (Wiley, 2021), vol 2, chap. 32, pp. 281-304.
413 [2] A. Hayashi, M. Nishihara, J. Matsuda, K. Sasaki, Polymer Electrolyte Fuel Cells (PEFCs), in: K. Sasaki, H.W. Li, A.
414 Hayashi, J. Yamabe, T. Ogura, S.M. Lyth (Eds), Hydrogen Energy Engineering: A Japanese Perspective, (Wiley,
415 2016), chap. 22, 301-312
416 [3] J. Zhao, X. Li, A review of polymer electrolyte membrane fuel cell durability for vehicular applications: Degradation
417 modes and experimental techniques, Energy Convers. Manag. 199 (2019) 112022.
418 https://doi.org/10.1016/j.enconman.2019.112022.
419 [4] Y. Wang, D.F. Ruiz Diaz, K.S. Chen, Z. Wang, X.C. Adroher, Materials, technological status, and fundamentals of
420 PEM fuel cells – A review, Mater. Today. 32 (2020) 178–203. https://doi.org/10.1016/j.mattod.2019.06.005.
421 [5] B. Smitha, S. Sridhar, A.A. Khan, Solid polymer electrolyte membranes for fuel cell applications — a review, J.
422 Membr. Sci. 259 (2005) 10–26. https://doi.org/10.1016/j.memsci.2005.01.035.
423 [6] Q. Li, R. He, J.O. Jensen, N.J. Bjerrum, Approaches and Recent Development of Polymer Electrolyte Membranes for
424 Fuel Cells Operating above, Chem. Mater., 15 (2003) 4896–4915. https://doi.org/10.1021/cm0310519.
425 [7] T. Bayer, B. V. Cunning, R. Selyanchyn, M. Nishihara, S. Fujikawa, K. Sasaki, S.M. Lyth, High temperature proton
426 conduction in nanocellulose membranes: Paper fuel cells, Chem. Mater. 28 (2016) 4805–4814.
427 https://doi.org/10.1021/acs.chemmater.6b01990.
428 [8] H. Nguyen, F. Lombeck, C. Schwarz, P.A. Heizmann, M. Adamski, H.F. Lee, B. Britton, S. Holdcroft, S. Vierrath, M.
429 Breitwieser, Hydrocarbon-based Pemion^{TM} proton exchange membrane fuel cells with state-of-the-art performance,
430 Sustain. Energy Fuels. 5 (2021) 3687–3699. https://doi.org/10.1039/d1se00556a.
431 [9] B. Hwang, S. Kondo, T. Kikuchi, K. Sasaki, A. Hayashi, M. Nishihara, Silicone-containing polymer blend electrolyte
432 membranes for fuel cell applications, J. Appl. Polym. Sci. 138 (2021) 1–13. https://doi.org/10.1002/app.50328.
433 [10] L. Christiani, K. Sasaki, M. Nishihara, Aliphatic SPI charge-transfer complex hybrid films for high temperature
434 polymer electrolyte membrane fuel cells, J. Appl. Polym. Sci. 135 (2018) 1–9. https://doi.org/10.1002/app.46087.
435 [11] B. Lafitte, P. Jannasch, Proton-conducting aromatic polymers carrying hypersulfonated side chains for fuel cell
436 applications, Adv. Funct. Mater. 17 (2007) 2823–2834. https://doi.org/10.1002/adfm.200700107.
437 [12] S. Feng, S. Kondo, T. Kikuchi, L. Christiani, B. Hwang, K. Sasaki, M. Nishihara, Development of a Heat-Treated
438 Polymer-Polymer Type Charge-Transfer Blend Membrane for Application in Polymer Electrolyte Fuel Cells, ACS
439 Appl. Energy Mater. 2 (2019) 8715–8723. https://doi.org/10.1021/acsaem.9b01697.

[13] Z. Long, K. Miyatake, High-Performance Fuel Cell Operable at 120 °c Using Polyphenlyene Ionomer Membranes with Improved Interfacial Compatibility, ACS Appl. Mater. Interfaces. 13 (2021) 15366–15372. https://doi.org/10.1021/acsami.1c04270.

[14] Y. yuan Zhao, E. Tsuchida, Y.K. Choe, J. Wang, T. Ikeshoji, A. Ohira, Theoretical studies on the degradation of hydrocarbon copolymer ionomers used in fuel cells, J. Memb. Sci. 487 (2015) 229–239. https://doi.org/10.1016/j.memsci.2015.04.005.

[15] J. Miyake, R. Taki, T. Mochizuki, R. Shimizu, R. Akiyama, M. Uchida, K. Miyatake, Design of flexible polyphenylene proton-conducting membrane for next-generation fuel cells, Sci. Adv. 3 (2017). https://doi.org/10.1126/sciadv.aao0476.

[16] S. Xu, M. Adamski, M. Killer, E.M. Schibli, B.J. Frisken, S. Holdcroft, Sulfo-Phenylated Polyphenylenes Containing Sterically Hindered Pyridines, Macromolecules. 52 (2019) 2548–2559. https://doi.org/10.1021/acs.macromol.8b02289.

[17] A.R. Motz, M.C. Kuo, J.L. Horan, R. Yadav, S. Seifert, T.P. Pandey, S. Galioto, Y. Yang, N. V. Dale, S.J. Hamrock, A.M. Herring, Heteropoly acid functionalized fluoroelastomer with outstanding chemical durability and performance for vehicular fuel cells, Energy Environ. Sci. 11 (2018) 1499–1509. https://doi.org/10.1039/c8ee00545a.

[18] S.H. Shin, A. Kodir, D. Shin, S.H. Park, B. Bae, Perfluorinated composite membranes with organic antioxidants for chemically durable fuel cells, Electrochim. Acta. 298 (2019) 901–909. https://doi.org/10.1016/j.electacta.2018.12.150.

[19] M. Breitwieser, T. Bayer, A. Büchler, R. Zengerle, S.M. Lyth, S. Thiele, A fully spray-coated fuel cell membrane electrode assembly using Aquivion ionomer with a graphene oxide/cerium oxide interlayer, J. Power Sources. 351 (2017) 145–150. https://doi.org/10.1016/j.jpowsour.2017.03.085.

[20] H. Lee, M. Han, Y.W. Choi, B. Bae, Hydrocarbon-based polymer electrolyte cerium composite membranes for improved proton exchange membrane fuel cell durability, J. Power Sources. 295 (2015) 221–227. https://doi.org/10.1016/j.jpowsour.2015.07.001.

[21] M. Danilczuk, F.D. Corns, S. Schlick, Visualizing chemical reactions and crossover processes in a fuel cell inserted in the esr resonator: Detection by spin trapping of oxygen radicals, nafion-derived fragments, and hydrogen and deuterium atoms, J. Phys. Chem. B. 113 (2009) 8031–8042. https://doi.org/10.1021/jp901597f.

[22] Z. Rui, J. Liu, Understanding of free radical scavengers used in highly durable proton exchange membranes, Prog. Nat. Sci. Mater. Int. 30 (2020) 732–742. https://doi.org/10.1016/j.pnsc.2020.08.013.

[23] M. Zatoń, J. Rozière, D.J. Jones, Current understanding of chemical degradation mechanisms of perfluorosulfonic acid membranes and their mitigation strategies: A review, Sustain. Energy Fuels. 1 (2017) 409–438. https://doi.org/10.1039/c7se00038c.

[24] M. Inaba, T. Kinumoto, M. Kiriake, R. Umebayashi, A. Tasaka, Z. Ogumi, Gas crossover and membrane degradation

in polymer electrolyte fuel cells, Electrochim. Acta. 51 (2006) 5746–5753. https://doi.org/10.1016/j.electacta.2006.03.008.

[25] G. Shi, D.A. Tryk, T. Iwataki, H. Yano, M. Uchida, A. Iiyama, H. Uchida, Unparalleled mitigation of membrane degradation in fuel cells: Via a counter-intuitive approach: Suppression of H2O2 production at the hydrogen anode using a Ptskin-PtCo catalyst, J. Mater. Chem. A. 8 (2020) 1091–1094. https://doi.org/10.1039/c9ta12023h.

[26] V.A. Sethuraman, J.W. Weidner, A.T. Haug, S. Motupally, L. V. Protsailo, Hydrogen Peroxide Formation Rates in a PEMFC Anode and Cathode, J. Electrochem. Soc. 155 (2008) B50-57. https://doi.org/10.1149/1.2801980.

[27] L. Du, V. Prabhakaran, X. Xie, S. Park, Y. Wang, Y. Shao, Low-PGM and PGM-Free Catalysts for Proton Exchange Membrane Fuel Cells: Stability Challenges and Material Solutions, Adv. Mater. 33 (2021) 1–18. https://doi.org/10.1002/adma.201908232.

[28] L. Du, C. Du, G. Chen, F. Kong, G. Yin, Y. Wang, Metal-Organic Coordination Networks: Prussian Blue and Its Synergy with Pt Nanoparticles to Enhance Oxygen Reduction Kinetics, ACS Appl. Mater. Interfaces. 8 (2016) 15250–15257. https://doi.org/10.1021/acsami.6b02630.

[29] A. Ohma, S. Suga, S. Yamamoto, K. Shinohara, Membrane Degradation Behavior during Open-Circuit Voltage Hold Test, J. Electrochem. Soc. 154 (2007) B757-760. https://doi.org/10.1149/1.2741129.

[30] J. Zhang, B.A. Litteer, W. Gu, H. Liu, H.A. Gasteiger, Effect of Hydrogen and Oxygen Partial Pressure on Pt Precipitation within the Membrane of PEMFCs, J. Electrochem. Soc. 154 (2007) B1006. https://doi.org/10.1149/1.2764240.

[31] Å. Nyflött, Ç. Meriçer, M. Minelli, E. Moons, L. Järnström, M. Lestelius, M.G. Baschetti, The influence of moisture content on the polymer structure of polyvinyl alcohol in dispersion barrier coatings and its effect on the mass transport of oxygen, J. Coatings Technol. Res. 14 (2017) 1345–1355. https://doi.org/10.1007/s11998-017-9937-2.

[32] M. Schalenbach, T. Hoefner, P. Paciok, M. Carmo, W. Lueke, D. Stolten, Gas Permeation through Nafion. Part 1: Measurements, J. Phys. Chem. C. 119 (2015) 25145–25155. https://doi.org/10.1021/acs.jpcc.5b04155.

[33] C.Y. Wong, W.Y. Wong, K.S. Loh, W.R.W. Daud, K.L. Lim, M. Khalid, R. Walvekar, Development of Poly(Vinyl Alcohol)-Based Polymers as Proton Exchange Membranes and Challenges in Fuel Cell Application: A Review, Polym. Rev. 60 (2020) 171–202. https://doi.org/10.1080/15583724.2019.1641514.

[34] T. Zhou, Y. Li, W. Wang, L. He, L. Cai, C. Zeng, Application of a novel PVA-based proton exchange membrane modified by reactive black KN-B for low-temperature fuel cells, Int. J. Electrochem. Sci. 14 (2019) 8514–8531. https://doi.org/10.20964/2019.09.16.

[35] T. Zhou, J. Zhang, J. Qiao, L. Liu, G. Jiang, J. Zhang, Y. Liu, High durable poly(vinyl alcohol)/Quaterized hydroxyethylcellulose ethoxylate anion exchange membranes for direct methanol alkaline fuel cells, J. Power Sources.

227 (2013) 291–299. https://doi.org/10.1016/j.jpowsour.2012.11.041.

[36] A.K. Sahu, G. Selvarani, S.D. Bhat, S. Pitchumani, P. Sridhar, A.K. Shukla, N. Narayanan, A. Banerjee, N. Chandrakumar, Effect of varying poly(styrene sulfonic acid) content in poly(vinyl alcohol)-poly(styrene sulfonic acid) blend membrane and its ramification in hydrogen-oxygen polymer electrolyte fuel cells, J. Memb. Sci. 319 (2008) 298–305. https://doi.org/10.1016/j.memsci.2008.04.004.

[37] J. Kim, K. Yamasaki, H. Ishimoto, Y. Takata, Ultrathin electrolyte membranes with PFSA-vinylon intermediate layers for PEM fuel cells, Polymers 12 (2020), 1730. https://doi.org/10.3390/POLYM12081730.

[38] S.K. Sharma, J. Prakash, J. Bahadur, M. Sahu, S. Mazumder, P.K. Pujari, Free volume and lamellar structure of poly vinyl alcohol-nanosized BaTiO3 composite: Positron annihilation and small angle X-ray scattering study, Eur. Polym. J. 84 (2016) 100–110. https://doi.org/10.1016/j.eurpolymj.2016.09.007.

[39] N.A. Peppas, D. Tennenhouse, Semicrystalline poly(vinyl alcohol) films and their blends with poly(acrylic acid) and poly(ethylene glycol) for drug delivery applications, J. Drug Deliv. Sci. Technol. 14 (2004) 291–297. https://doi.org/10.1016/s1773-2247(04)50050-3.

[40] M.K. Mohanapriya, K. Deshmukh, K. Chidambaram, M.B. Ahamed, K.K. Sadasivuni, D. Ponnamma, M.A.A. AlMaadeed, R.R. Deshmukh, S.K.K. Pasha, Polyvinyl alcohol (PVA)/polystyrene sulfonic acid (PSSA)/carbon black nanocomposite for flexible energy storage device applications, J. Mater. Sci. Mater. Electron. 28 (2017) 6099–6111. https://doi.org/10.1007/s10854-016-6287-2.

[41] S. Jo, K.R. Yoon, Y. Lim, T. Kwon, Y.S. Kang, H. Sohn, S.H. Choi, H.J. Son, S.H. Kwon, S.G. Lee, S.S. Jang, S.Y. Lee, H.J. Kim, J.Y. Kim, Single-Step Fabrication of Polymeric Composite Membrane via Centrifugal Colloidal Casting for Fuel Cell Applications, Small Methods. 5 (2021) 1–10. https://doi.org/10.1002/smtd.202100285.

[42] A. Kusoglu, S. Savagatrup, K.T. Clark, A.Z. Weber, Role of mechanical factors in controlling the structure-function relationship of PFSA ionomers, Macromolecules. 45 (2012) 7467–7476. https://doi.org/10.1021/ma301419s.

[43] J.P. Melchior, T. Bräuniger, A. Wohlfarth, G. Portale, K.D. Kreuer, About the Interactions Controlling Nafion's Viscoelastic Properties and Morphology, Macromolecules. 48 (2015) 8534–8545. https://doi.org/10.1021/acs.macromol.5b01559.

[44] J. Tang, W. Yuan, J. Wang, J. Tang, H. Li, Y. Zhang, Perfluorosulfonate ionomer membranes with improved through-plane proton conductivity fabricated under magnetic field, J. Memb. Sci. 423–424 (2012) 267–274. https://doi.org/10.1016/j.memsci.2012.08.023.

[45] S.H. Yun, S.H. Shin, J.Y. Lee, S.J. Seo, S.H. Oh, Y.W. Choi, S.H. Moon, Effect of pressure on through-plane proton conductivity of polymer electrolyte membranes, J. Memb. Sci. 417–418 (2012) 210–216. https://doi.org/10.1016/j.memsci.2012.06.041.

[46] J.E. Hensley, J.D. Way, S.F. Dec, K.D. Abney, The effects of thermal annealing on commercial Nafion® membranes, J. Memb. Sci. 298 (2007) 190–201. https://doi.org/10.1016/j.memsci.2007.04.019.

[47] M. Glassman, A. Omosebi, R.S. Besser, Repetitive hot-press approach for performance enhancement of hydrogen fuel cells, J. Power Sources. 247 (2014) 384–390. https://doi.org/10.1016/j.jpowsour.2013.08.090.

[48] D. DeBonis, M. Mayer, A. Omosebi, R.S. Besser, Analysis of mechanism of Nafion® conductivity change due to hot pressing treatment, Renew. Energy. 89 (2016) 200–206. https://doi.org/10.1016/j.renene.2015.11.081.

[49] J. Zhang, H.A. Gasteiger, W. Gu, Electrochemical Measurement of the Oxygen Permeation Rate through Polymer Electrolyte Membranes, J. Electrochem. Soc. 160 (2013) F616–F622. https://doi.org/10.1149/2.081306jes.

[50] New Energy and Industrial Technology Development Organization, PEFC Evaluation Project - Cell Evaluation and Analysis Protocol Guideline. https://www.nedo.go.jp/content/100537904.pdf (Accessed 16 February 2022)

[51] U.S Department of Energy, DOE Technical Targets for Polymer Electrolyte Membrane Fuel Cell Components. https://www.energy.gov/eere/fuelcells/doe-technical-targets-polymer-electrolyte-membrane-fuel-cell-components. (Accessed 16 February 2022)

[52] A. Ohma, S. Yamamoto, K. Shinohara, Analysis of Membrane Degradation Behavior During OCV Hold Test, ECS Trans. 11 (2007) 1181–1192. https://doi.org/10.1149/1.2781032.

[53] M. Yandrasits, M. Lindell, D. Peppin, A. Komlev, S. Hamrock, G. Haugen, E. Fort, K. Kalstabakken, Chemical Stability of Perfluorobis(sulfonyl)imide-Acid (PFIA) Ionomers in Open Circuit Voltage (OCV) Accelerated Test Conditions, J. Electrochem. Soc. 165 (2018) F3261–F3270. https://doi.org/10.1149/2.0301806jes.

[54] S.H. Bossmann, E. Oliveros, S. Göb, M. Kantor, A. Göppert, L. Lei, P.L. Yue, A.M. Braun, Degradation of polyvinyl alcohol (PVA) by homogeneous and heterogeneous photocatalysis applied to the photochemically enhanced Fenton reaction, Water Sci. Technol. 44 (2001) 257–262. https://doi.org/10.2166/wst.2001.0300.